Perched Landing Manoeuvres with a Variable Sweep Wing UAV

Colin Greatwood[a,1,*], Antony Waldock[b], Thomas Richardson[a,3]

[a]*Department of Aerospace Engineering, University of Bristol, Queens Building, University Walk, Bristol, BS8 1TR*
[b]*BMT Defence Services*

Abstract

A variable sweep wing UAV is developed utilising off the shelf components with a custom mechanism for the wing box. The movement of the wing sweep in flight enables large pitching moments suitable for performing perching manoeuvres. Wind tunnel data is presented that confirms the favourable characteristics expected from sweeping the wing and achieving high pitch rates. Whilst only small sweep changes are required during flight, the design allows up to 30° forward sweep for significant pitching moments during the flare.

A new collection of controllers is developed based on observations from similar landing techniques performed by birds and hang-gliders onto flat ground. The three-stage landing process takes the aircraft along an approach path, through a roundout procedure during which airspeed decays and concludes with rapid pitch up. Flight test results are presented during which it is found that the airspeed can be reduced to, on average, under $3m/s$ in the final moments before landing - well below the stall speed of $9m/s$.

1. Introduction

The topic of variable geometry and morphing aircraft has recently attracted a lot of attention due the potential to improve aircraft performance and widen their flight envelope. Concepts such as morphing wing tips can offer important fuel weight reductions [1] in passenger aircraft. For Unmanned Air Vehicles (UAVs) it has also been shown that morphing can be used to trade flight performance for handling qualities in flight through the use of a variable gull-wing for example [2]. One of the key advantages that the work in this area has shown is a multi-role capability, whereby changing the aircraft structure during flight could improve agility [3] and enable multi-role capabilities, as highlighted by several surveys on the subject, *e.g.* Refs. [4] and [5].

The UAV presented in this study is capable of flying like a conventional fixed wing aircraft, but has been designed to allow it to perform landings onto small landing sites though perching type manoeuvres. In general, the goal of the perching manoeuvre is to bring the velocity of the aircraft to close-to-zero speeds just before touching down. Perching or landing with low ground speeds will remove the requirement for the typical infrastructure required such as runways, hooks or nets. Perching is therefore an attractive

*Corresponding author
Email addresses: colin.greatwood@bristol.ac.uk (Colin Greatwood), awaldock@bmtdsl.co.uk (Antony Waldock), thomas.richardson@bristol.ac.uk (Thomas Richardson)
[1]Senior Research Associate
[2]Principal Systems Analyst
[3]Senior Lecturer

solution to landing in unprepared or difficult landing sites and even for emerging applications like "perch and stare".

Perching is a difficult control problem as it requires the aircraft to effectively stop flying and be close to stationary (zero forward and vertical speed) just before it touches down at the landing location. If an aircraft was to fly into its landing site at its minimum (stall) airspeed then it would likely damage itself, hence why parachutes or nets are often used to slow the aircraft down, *e.g.* Refs. [6, 7]. Typically only much smaller (sub 10 gram) UAVs would be able to perch onto an unprepared landing site with simple control strategies; these aircraft can use mechanical intelligence and compliance during landing [8, 9, 10]. Therefore, UAVs of a scale similar to birds have been demonstrated to take advantage of deep stall for aerodynamic breaking whilst landing in steep descents [11, 12], although impact speeds may still require any delicate payloads to be packaged carefully.

The problem of designing UAVs to perform perched landings has been previously demonstrated, *e.g.* in Refs. [13, 14, 15], but often the landing site (perch) has been raised above the surrounding ground allowing the aircraft to swoop or *undershoot* from below the perch to reduce airspeed. Additionally, a lot of the work in this area has taken advantage of accurate, high speed Vicon motion capture systems that use a series of calibrated cameras to precisely track the position of the aircraft.

It has been found that installing aircraft with higher thrust-to-weight ratios can reduce the required undershoot [16] as can the use of thrust vectoring [17]. In the limit a thrust to weight ratio greater than one would enable a perch landing by simply landing in the hover; furthermore taking off vertically from the perch is then also possible [18, 19]. Instead, we tackle to problem of landing with *zero* undershoot (*i.e.* on flat ground) with a more bio-inspired approach of landing with the throttle turned off. Perching onto fixed structures is, however, left until future work when integration of additional sensing such as computer vision could help with localisation, such as that demonstrated by Thomas et al. where monocular vision is used to steer swooping trajectories [20].

Both birds and hang-gliders are excellent examples of un-powered perching aircraft and provide some of the inspiration in the control design implemented in this paper. The hang-glider will perform a conventional approach at speeds above the stall speed. When close to the ground in the round-out phase of landing, airspeed is allowed to decay as the pilot maintains a constant height over the ground until close to the stall speed. At that point the pilot initiates a rapid pitch-up manoeuvre which delays stall until high incidence angles. This enables high lift coefficients to be achieved such that the airspeed can be reduced to values close to those within the capabilities of the pilots legs. Indeed with practise landings with zero ground speed can be consistently achieved. Some birds have demonstrated more three dimensional perching approaches and researchers have found that the inclusion of lateral dynamics in optimising perch trajectories can reduce the required undershoot [21]. The complex inclusion of lateral dynamics on the landing control is, however, considered outside the scope of the current paper.

For a standard airframe configuration perching is difficult because the aircraft is unable to generate large enough pitching moments, which has been found to be a key factor in minimising required undershoot [22]. Designing in a small static margin, or even an unstable aircraft could improve the ability to perch but could negatively impact the stability during flight. In fact researchers have demonstrated

experimentally that it is possible to perform perching manoeuvres [13] when the aircraft is configured to generate the large pitching moments from suitable static margins and tail control surface area.

Figure 1: Bixler 2 Airframe, fitted with variable sweep and twist mechanisms

The approach to generating the large pitching moments required is tackled here using variable wing sweep, which enables the aircraft to change the centre of pressure relative to the centre of gravity during flight. This is very similar to the way that many birds control their pitch attitude and undertake perching manoeuvres. It would be possible to build a mechanism to shift the centre of mass by adjusting the battery position for example, much like a hang-glider pilot moving his body; instead we take inspiration from the wing sweep degree of freedom used by birds for pitch control. Previous work in this area has shown that using wing sweep for pitch control on a UAV of this size is a viable alternative to elevator control [23], with recommendations to use such a mechanism for perching manoeuvres. Numerical optimisation of perching trajectories for a UAV with a similar wing sweep mechanism also confirms [24] the benefits of this increased pitch control authority. The aircraft designed and built for evaluating these manoeuvres is shown in Figure 1 and details on the design are presented in Section 2.

The pitch rates achievable through sweeping the wing forward are significantly higher than those from the UAV's traditional elevator. The wing is therefore able to further benefit from the dynamic effects of pitching up quickly, which cause the wing to stall at higher angles of attack than if pitched up slowly. Wind tunnel results presented in Section 3.2 illustrate the additional lift made available through large pitch rates.

In the work presented here inspiration is taken from the approach of the hang glider pilots and birds that perform landings onto ground level targets. A UAV is developed to fly outdoors using low cost on-board sensors for control feedback. Section 2 describes the variable sweep aircraft that was designed to evaluate the perched landings. The flight dynamics of the aircraft are then explored in Section 3, providing further insight into the suitability of the sweeping design for perched landings. Wind tunnel data is also collected to back up the theory. Section 4 then presents the various control laws that are constructed for taking the aircraft from being lined up for landing, through the approach all the way to the final flare in landing. Finally flight test results are presented in Section 5.

2. Airframe Design

In order to accelerate the development of the concepts described in this study, a Commercial Off The Shelf (COTS) airframe was modified (Fig. 1). The "Bixler 2" airframe is a 1.5 metre wingspan model aircraft made from expanded polyolefin foam and as standard does not have any sweep on the wing. A custom wingbox was designed to allow the sweep angle of the wing to be varied between $-20°$ (aft) and $30°$ (forward). Varying the wing sweep in flight can be used for pitch control due to shifting the centre of gravity relative to the centre of pressure, as will be described in further detail in Section 3.

The wing tips of the Bixler were modified to allow them to pitch as entire outer wing sections about the quarter chord point. The moving wing tips can be considered as separate lifting bodies that cause a rolling moment due to asymmetric lift during differential deflection from one side to the other. Moving the tips as separate sections is easy to implement on the existing wing, but could for small deflections be seen as crudely approximating the effects of wing twist or warping. Additionally, rotating the wing tips symmetrically would achieve some of the benefits found from a wing with washout. Specifically, at high angles of attack during perching manoeuvres it is important to avoid stalling of the wing tips and potentially correct small roll perturbations. By reducing the incidence of the wing tips through these manoeuvres roll control could be expected to be more effective.

The main modification to the airframe was the custom wingbox, which must support the wing flight loads whilst enabling the wings to be swept between $20°$ backwards and $30°$ forwards. The wingbox mechanism, shown in Figure 2(d) consists of: 2mm Carbon fibre plates top and bottom to support the pins that the wings pivot about; A central box that supports torsional loads and provides rails that support wing bending loads; Side plates that support the servo actuator and an aft control horn linkage. These side plates are supported in the fuselage by three carbon pins, which fit through the holes seen in Figure 2(b).

The design allows the wing sweep servo to be located close to the centre of gravity and minimise its impact on the aircraft's balance and inertia. Furthermore, the rear control horn linkage transfers all longitudinal loads from the wing roots to pure rotational loads for the servo actuator. Any significant loads or impacts on the wing will be supported by the bearing about which the rear control horn linkage rotates.

The wingbox mechanism was also designed to be lightweight, but more importantly to be robust to withstand the potentially heavy landings possible during experimental testing. The mechanism therefore has a weak link in the design; should one or both of the wings be knocked back during a bad landing the plastic servo horn will break first rather than gears inside the servo or a hard to service part of the mechanism. A small service hatch in the fuselage provides access to replace this servo horn.

Figure 2(c) shows the plywood box section that is embedded in the foam of the wings to transfer bending loads to the root of the wing. On the inboard side of the spar box (RHS of figure) a ball link push-rod is connected, extending to the rear control horn in the mechanism. The ball bearing installed just inboard of the linkage runs along the rails of the central section of the wingbox, providing bending moment support in addition to the pivot pin. The pivot pins are constructed from 10mm carbon fibre tubes. Thrust bearings are installed on the pins between the spar boxing and the wingbox carbon fibre

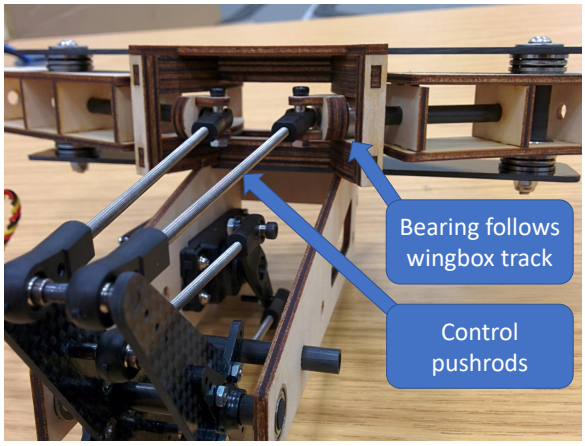

(a) Wingbox variable sweep mechanism, viewed from rear

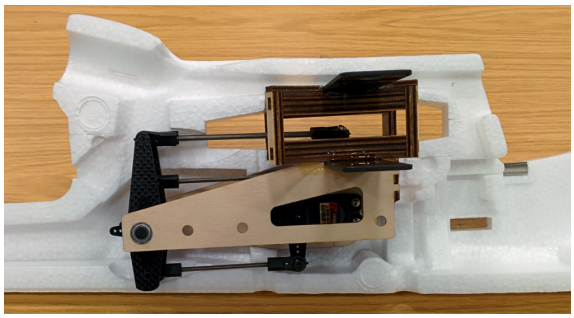

(b) Wingbox in fuselage half

(c) Spar boxing for wing root

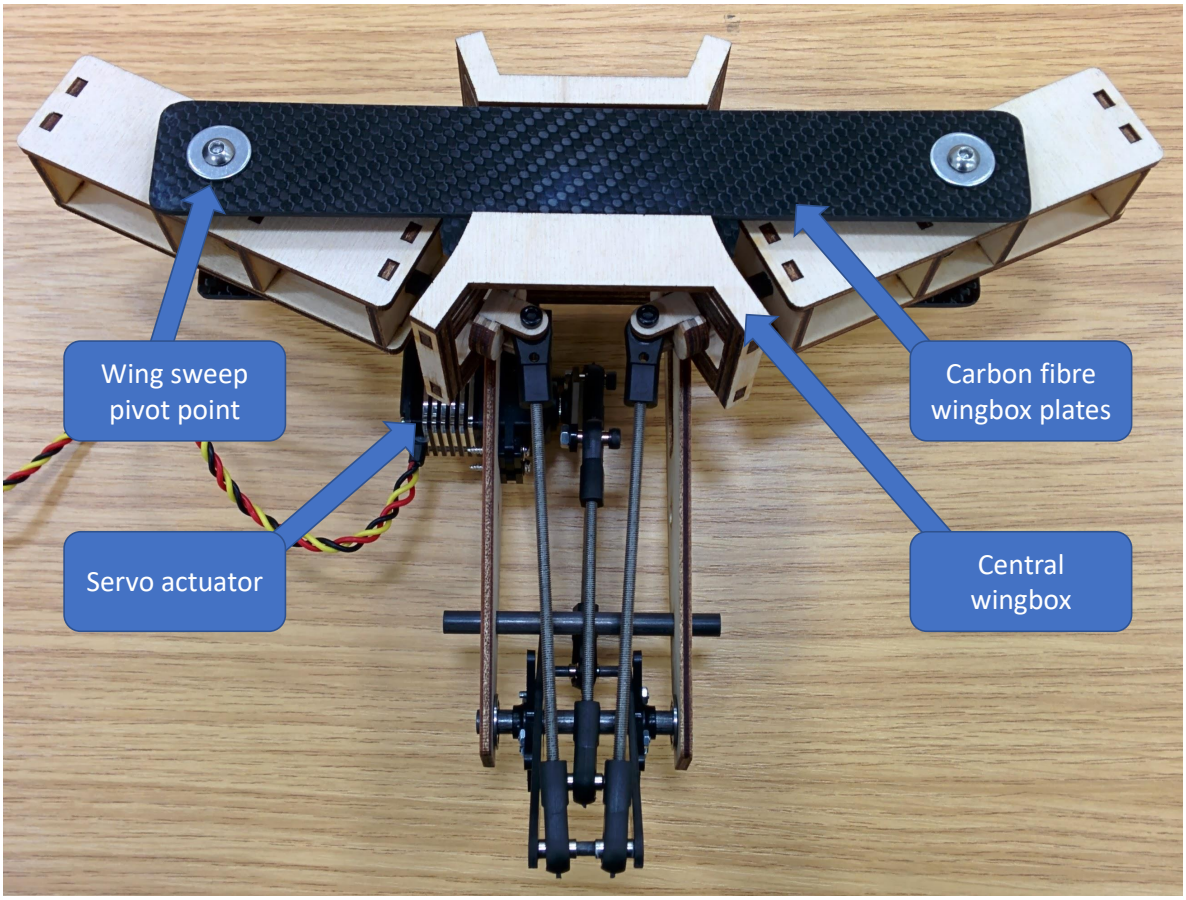

(d) Wingbox variable sweep mechanism, viewed from above

Figure 2: Variable wing sweep mechanism components. Spar boxing (c) is embedded into wing root and enables wing sweep control, pivoting inside the wingbox. Control pushrod linkage system transfers fore/aft forces into rotational loads at servo actuator.

plates and enable very free movement under high load conditions.

The outer 250mm sections of the wing was cut chord-wise to create discrete wing tip sections capable of pitching up and down. A 4mm carbon fibre rod was installed protruding from the main wing spar to support the wingtips. Ball bearings installed in the wingtips then enable free movement under flight loads. Servos are installed in the top of the wing and articulate the wingtips using a pushrod assembly. These servos are connected to the flight controller in such a way that both differential and symmetric movement are possible for roll control and washout control.

3. Flight Dynamics

3.1. Longitudinal Response

The variable wing sweep may be used for pitch control of the aircraft. As the wings sweep forward and aft the centre of lift and centre of mass both move. The centre of lift, however, moves the furthest out of the two from the original centre of mass. This shifting of the centre of lift relative to the centre of mass leads to a positive pitching moment as the wings sweep forward and a negative moment for aft sweep.

Figure 3 shows the pitching moment versus angle of attack for the aircraft with different wing sweep settings from wind tunnel tests. It can be seen that plus or minus five degrees wing sweep provides comparable pitching moments to the full plus or minus ten degrees elevator deflection for most positive angles of attack. As one might expect sweeping the wings forward will reduce the pitch stability, however, the plot shows that even with ten degrees forward sweep the aircraft has positive pitch stability. The reduction in pitch stability is an advantage in the perch manoeuvre though, as it means the control authority will be increased during the critical phase when a high pitch rate is desired. Figure 3 also shows that at five degrees angle of attack, which is required for 1g flight at 8.5m/s, the elevator cannot produce a positive pitching moment yet sweeping the wing forward will.

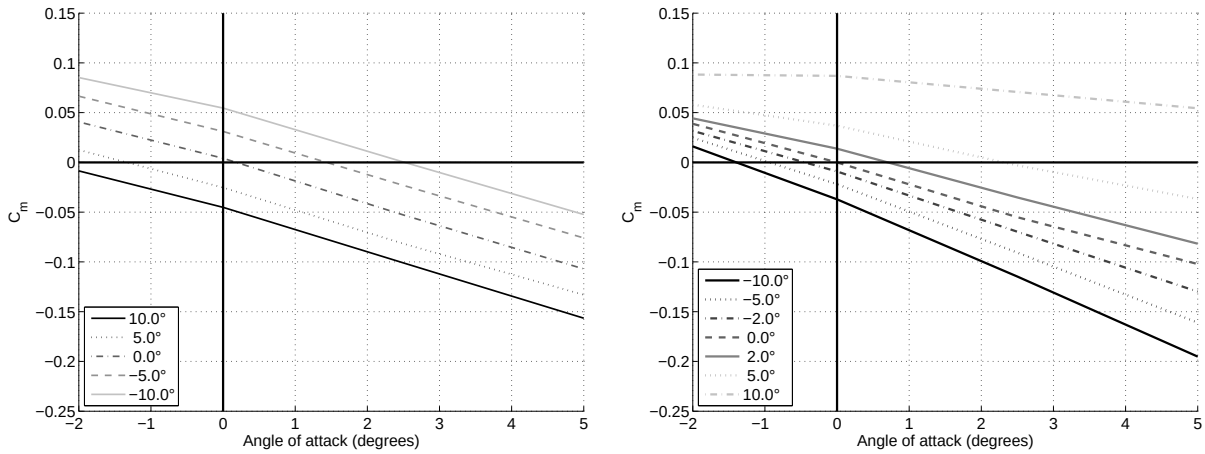

(a) Varying elevator setting angles, sweep fixed

(b) Varying sweep setting angles, elevator fixed

Figure 3: Pitching moment versus angle of attack, demonstrating sweep control can be used instead of elevator; furthermore pitch remains controllable at higher angles of attack when using wing sweep for control

3.2. Dynamic Response

One of the drivers for selecting a variable sweep wing is the ability to generate large pitching moments at low speeds, as discussed in the previous section. When a wing pitches up at high rates the angle at which it stalls can be delayed, enabling it to generate a larger $C_L^{\max}$. The larger $C_L^{\max}$ is useful in the final moments before landing as the aircraft can continue flying at a lower airspeed and therefore touch down with a lower forward velocity. This rapid pitch up in the final moments is what we refer to here as a perching landing. Figure 4 shows the lift curve slope for the sweep wing aircraft for different pitch rates, demonstrating the effect of the delayed stall. The plot shows the effects of pitch rate for both an unswept and fully forward swept wing. The forward swept wing in general appears to generate a marginally smaller $C_L^{\max}$ and a slightly less abrupt stall.

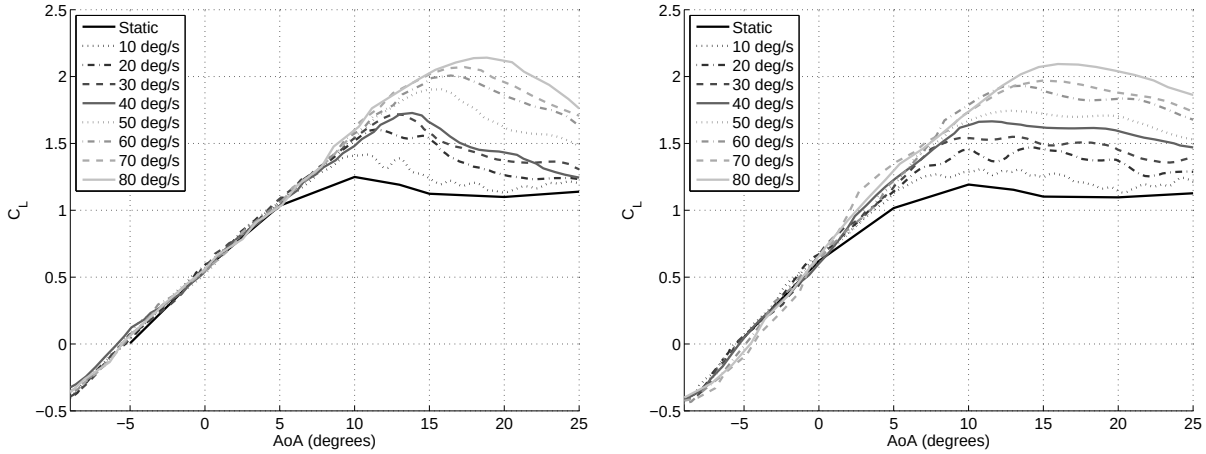

(a) Neutral sweep angle

(b) Wings swept forwards 30°

Figure 4: Lift curve slope for different pitch rates, tested at 8m/s airspeed

3.3. Roll Response

During high angle of attack perching manoeuvres it is desirable to avoid stalling of the wing tips, which may be mitigated by adding washout to the wing. The UAV designed and built for this work has variable incidence wing tip controls that can be used differently for roll response and symmetrically for variable washout. The wing could therefore have very little or no washout during cruise flight for a more efficient lift distribution and then increased washout during the landing phase.

In addition to tip stalling, roll reversal is a real risk at high angles of attack, especially if the incidence of a wing tip is increased beyond the stall. Figure 5 shows the roll response from varying the wing tip positions during a wind tunnel test at 10m/s. The wing tips were commanded to move equal and opposite amounts on each side for roll control and the resulting rolling moments for rolling both left and right are plotted. The results are plotted over a range of AoAs for two different wing sweep settings. When the wing sweep is neutral the entire wing was found to stall at around 10° AoA, after which the roll control can also be seen to reverse (Fig. 5(a)). In the second half of the plot the roll control is shown, but with a symmetric wing tip deflection (washout) superimposed. With washout included, the figure shows that roll control is still effective at 30° AoA, well beyond the point at which the main wing stalled.

The same test for roll control was performed with forward sweep introduced (Fig. 5(b)). The forward sweep causes the roll reversal to occur much sooner at less than half the AoA compared to zero sweep. Washout improves the response, but roll reversal still occurs at high AoAs. A greater range of available washout could delay this further.

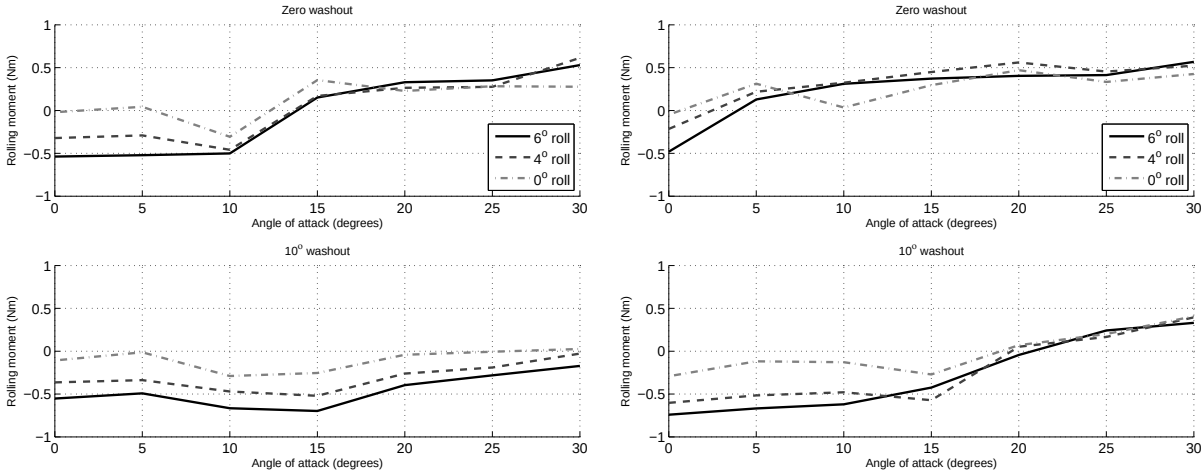

(a) Wing sweep fixed at 0°

(b) Wing sweep fixed at 20° forward

Figure 5: Roll response vs angle of attack - both with and without symmetric wing tip washout

4. Flight Control

A Pixhawk [25] flight controller unit was installed on the UAV running version 3.22 of the ArduPlane [26] autopilot software. The ArduPlane software is an open source project, enabling developers and researchers to modify the flight control laws as required. The software has automatic waypoint following built into it using a cascaded PID (proportional-integral-derivative) control structure.

Roll and pitch angles are tracked by ArduPlane's inner loop PID controller, which output commands to the roll and pitch channels. This inner loop may be tested by entering the "Fly-By-Wire A" mode (FBW-A) where roll and pitch angles are commanded through stick positions on the pilot's transmitter. Typically the pitch control channel would be the elevator, but in this case the wing sweep was connected instead. From the observed pitching moment response in Figure 3, it was decided that the difference between sweeping and elevator angle changes for small changes was not significant enough to require altering the control structure. Additionally, the wing tips were connected to the roll control channel instead of the ailerons. The FBW-A controller was therefore not modified and controlled pitch using wing sweep and roll using asymmetric wing tip deflection.

Outside the FBW-A loop the waypoint navigation tracks changes in heading using a proportional controller and altitude rate using a Total Energy Control System (TECS), based on previous work on total energy principles [27]. The change in desired heading is calculated using an L1 navigation controller [28] and the altitude rate is calculated from the gradient between the UAV's current position and next waypoint. Further information on the construction of ArduPlane's control laws may be found on the software's wiki page [29].

The ArduPlane software includes the capability for automatic landing, which continues to be improved as new versions of the software are released. The landing controllers, however, are designed for typical fixed wing designs landing on flat ground such as runways. The eventual goal here is instead to perform pitch up landings with high positional accuracy, such as onto a fixed structure. The development and flight tests in this study, however, are restricted to landing on flat surfaces but with a sharp pitching up manoeuvre at the end to achieve a close to zero forward velocity. Additionally, the aircraft needs to maintain a small height above the ground prior to this final pitch up manoeuvre whilst the airspeed decays sufficiently. The proposed landing control law is split into three discrete phases: approach, roundout and flare, which are illustrated in Figure 6 and detailed in the following sections.

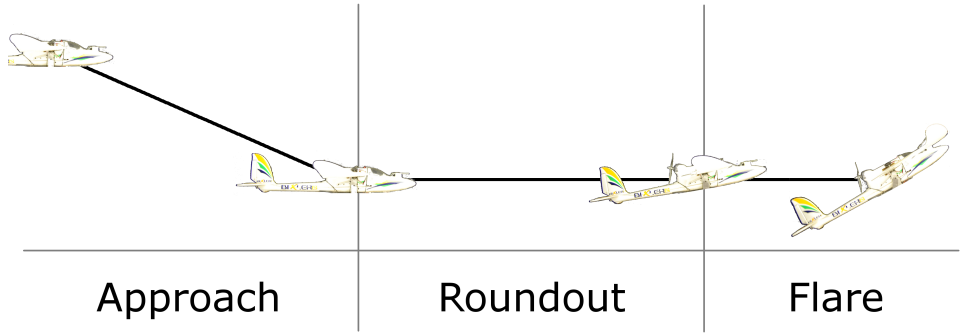

Figure 6: Three part landing process

4.1. Approach Controller

The job of the approach controller is to take the UAV from a position lined up with the landing site - from a few tens of metres up and of the order of 100m away - down to a position close to the ground and ten or twenty metres from the landing site. The final speed and position of the UAV at the end of the approach is critical as it will directly contribute to the accuracy of the final touch-down. Ideally the speed would be within a few metres a second of the target airspeed so that the energy of the vehicle is within a limited range and the work required by the roundout controller to successfully arrive at the final location with the right speed is minimal.

Typically the approach to a landing in ArduPlane would be handled by the TECS controller. The TECS controller is quite difficult to tune due to the large set of parameters that require tuning mostly by hand, along with estimates of performance metrics such as maximum climb rate and minimum sink rate. Although previous research has shown that a TECS control law could be tuned through eigenstructure assignment [30], this study instead implements a simpler control law using the technique described in Example 4.6-4 of Ref. [31].

A single input single output controller is used to control the airspeed during the descent. Airspeed is measured from the pitot tube and the throttle is adjusted from its cruise set-point via a proportional feedback term. A separate controller pitches the aircraft by sending pitch demands through the FBW-A controller to drive it back onto the commanded glide-slope. The geometry of the glide-slope is shown in Figure 7, where the current aircraft position $P(t_1)$ is compared against a point projected along the

current glide-slope at some point in the future $P(t_2)$. The perpendicular distance between the desired glide-slope and $P(t_2)$ is taken as the distance error d. A PD controller is used to drive the error d to zero and hence guide the aircraft along the glide-slope. Whilst it is difficult to measure d directly, $\dot{d}$ can be computed using the aircraft velocity and flight path angle error. This derivative is then integrated in order to determine d. Further details of the glide slope geometry are given in Ref. [31].

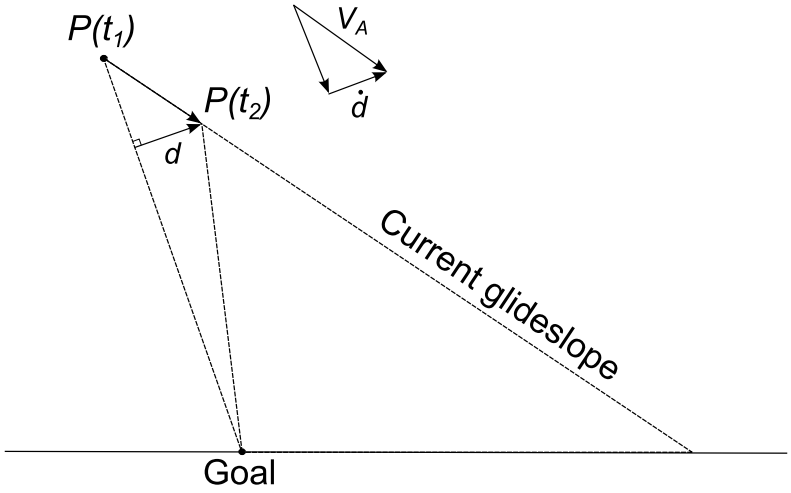

Figure 7: Glide-slope geometry, schematic from Example 4.6-4 of Ref. [31]

4.2. Roundout Controller

The roundout controller handles the transition from the approach controller and aims to maintain a given altitude above the ground whilst decelerating ready for the final flare. The throttle is typically closed and aircraft is pitched in order to maintain altitude whilst losing airspeed.

The roundout controller is outlined in Figure 8. The inputs to the roundout controller are a commanded height and throttle setting (typically zero). The roundout controller utilises the autopilot's inner loop attitude controller (FBW-A) to control the aircraft's roll and pitch angles. Around the FBW-A controller the L1 navigation controller commands a roll angle that keeps the aircraft on track for the touchdown location, although this target roll angle is now saturated to $\pm 5^\circ$ to avoid any significant manoeuvring. The commanded pitch angle is computed from the roundout controller using a PID controller on height above ground plus a proportional feedback on airspeed.

The roundout controller heavily relies upon an accurate estimate of how high the vehicle is above the ground. An onboard pressure altimeter is used for most of the flight for altitude estimates, but is subject to drift and inaccuracies in height above ground may arise if the flying site is on a gradient for example. To achieve a reliable and accurate height estimate an active ranging sensor is recommended. In the work presented here an ultrasonic sensor was fitted; this had a limited range of 7m, which meant that handling the transition between using the barometric altitude and measured height required careful consideration. It is important sudden spikes do not enter the control system as a result of the ranging sensor beginning to return valid readings. To reduce the effect of switching between sensor signals the vertical speed *h_dot* in Figure 8 only uses barometric measurements.

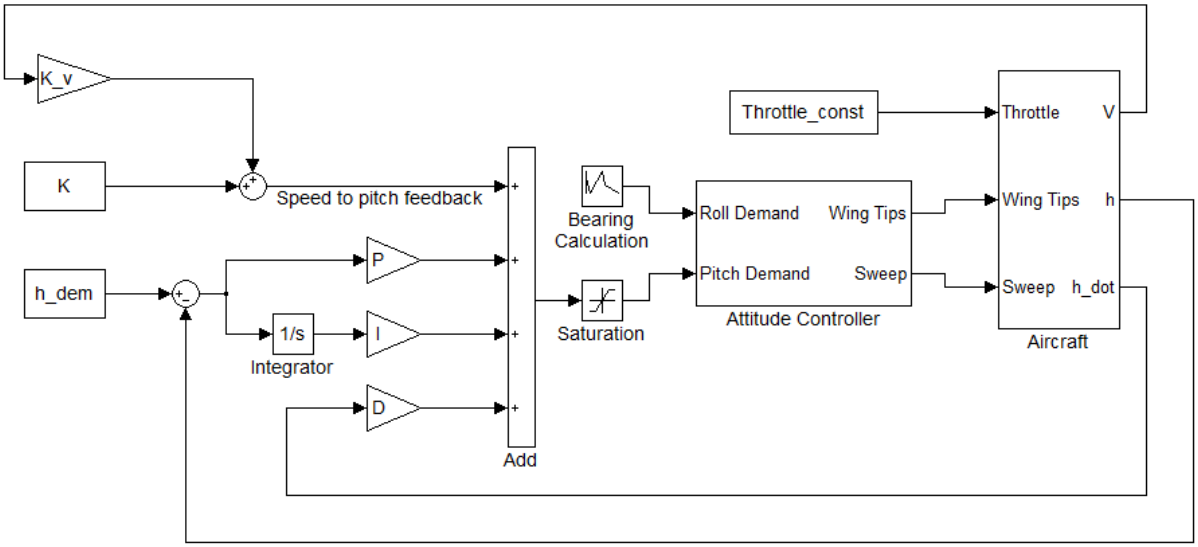

Figure 8: Outline of roundout control law

The P, I and D control gains for maintaining altitude during the roundout were tuned experimentally through trials at altitude and the final values are given in Table 1. The integral term was initially tuned to 0.8. With these gains it was then possible to perform a roundout without losing more than a couple of metres and the speed feedback gains could be determined. By observing the aircraft's pitch angle as it lost airspeed it was possible to determine approximately what pitch angle feedback term should be used. Figure 9 shows three roundout manoeuvres, plotting pitch angle against airspeed; the line of best fit suggests that the gains for K and K_v should be $36°$ and $-2.75°s/m$ respectively. The data below $9m/s$ is ignored during the fitting as at this speed the aircraft would be close to the stall and control would be handed over to the flare controller. The stall can be seen in the data as the pitch angle drops off rapidly due to the stall. Finally, upon setting these velocity feedback gains it was found that good performance was achieved with the integral term reduced to zero.

Gain	Value
P	8
I	0
D	12
K	$36°$
K_v	$-2.75°s/m$

Table 1: Roundout controller gains

In order to deliver the aircraft at the correct location for touch-down the rate of airspeed decay should be controlled to account for inaccuracies in entry speed and variations in wind conditions. It is anticipated that this airspeed decay would be controlled via a drag generation device, but this must be left to future work where further developments will improve repeatability in final touch down location.

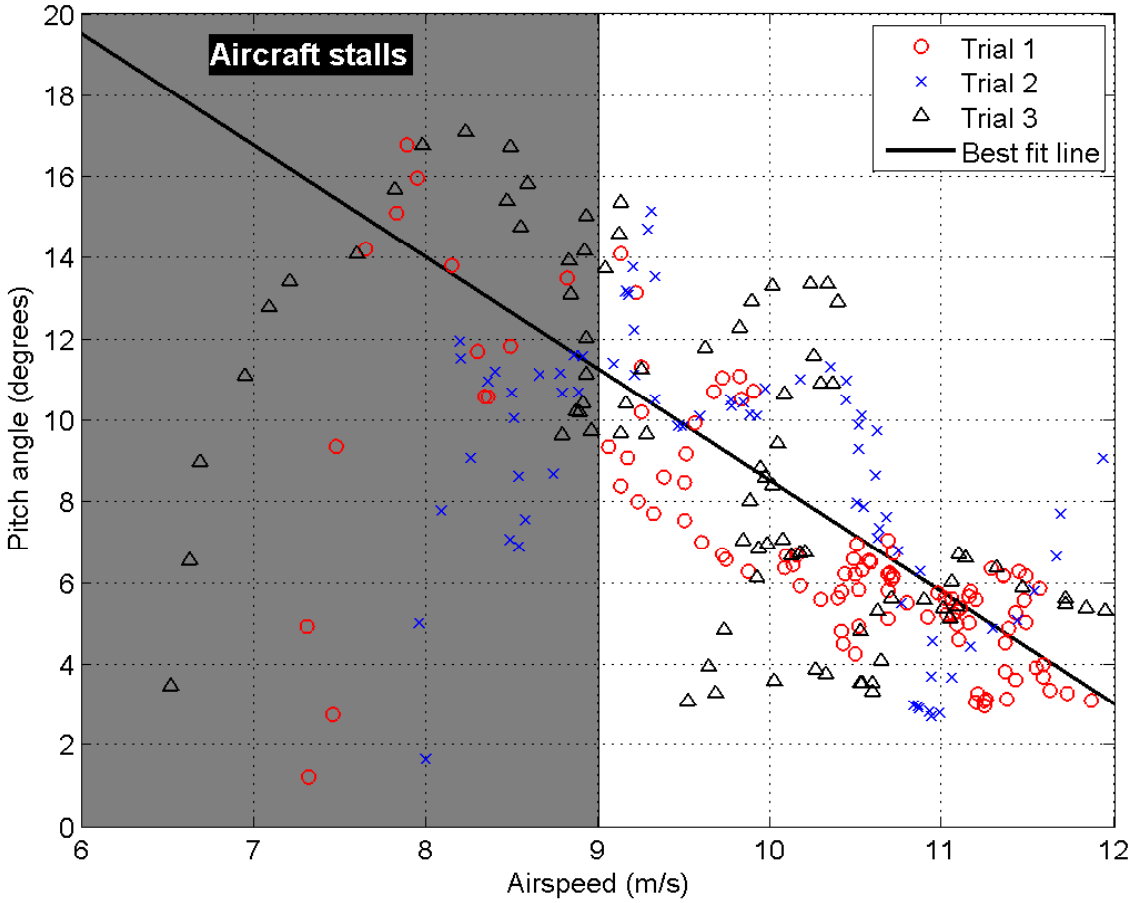

Figure 9: Pitch angles required to maintain altitude for different airspeeds

4.3. Flare Controller

Once the roundout controller has bled enough airspeed such that the aircraft is just about to stall the flare controller is engaged. The flare controller then commands a dynamic pitching up manoeuvre that keeps the aircraft airborne whilst the airspeed is driven to near zero.

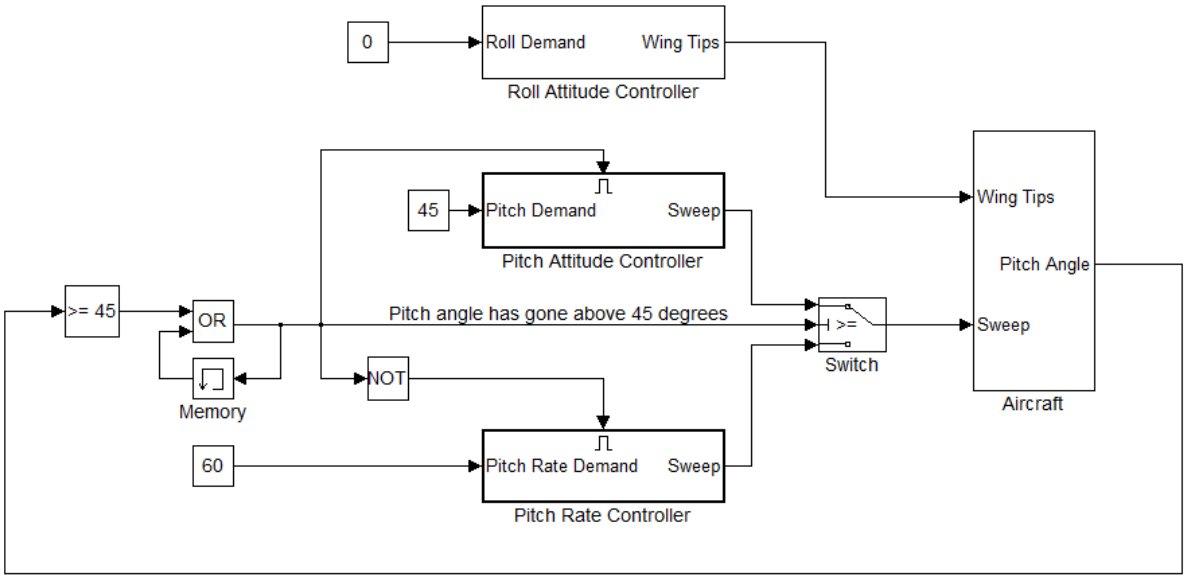

Figure 10: Outline of flare control law

The flare controller drives the roll angle to zero through the FBW-A controller in order to keep the wings level. Initially the pitch *rate* is commanded to accelerate to $60°/s$ using the autopilot's rate mode controller. Once the aircraft reaches a pitch angle of 45° it is then commanded to hold the same attitude of 45° by switching from the pitch rate controller into the FBW-A attitude controller. The 45° pitch hold is desirable as it is thought to maintain a balance between keeping a high angle of attack through the final stages of the landing, whilst not lifting the nose up too high and potentially causing damage to the aircraft on touch down. A photo of the aircraft performing the flare is shown in Figure 11 where successive frames from video footage have been superimposed to illustrate the motion. The photo shows the 45° attitude achieved at which point the pitch hold was been engaged, forward speed was low and the touch-down near the blue mat occurs moments later.

It is critical that the entry to the flare controller is both at a low altitude and with the aircraft already close to the stall. If the altitude is high then the aircraft will fall from that high altitude and potentially damage itself. If the aircraft is flying too fast then the rapid pitch-up will result in an upwards trajectory, again causing it to fall from a high altitude. If the aircraft is flying too slowly then it will fail to achieve the high pitch attitude and it will "mush" into the ground with greater forward velocity.

5. Landing Flight Test Results

This section presents flight test results for five separate landings that were carried out using the three control laws presented in the previous section. The aircraft was flown by the autopilot using the

Figure 11: Aircraft in final moments before landing, performing flare pitch-up

already available controllers (although configured to pitch via sweep and roll via wing tip deflection) automatically to a waypoint at 25m altitude and in line with the landing spot. After reaching the waypoint the autopilot switched over to the new control laws, starting with the approach.

Figure 12 shows the trajectory followed for each of the five approaches flown. The variation in initial altitude is immediately obvious, illustrating the variability of the entry conditions to the landing process from the stock automatic control. One of the key goals of the approach controller is to reduce this variability before the throttle is shut during the roundout phase. Indeed, by the end of the approach the spread in altitude and airspeed is greatly reduced.

Control was switched to the roundout controller upon reaching within ten metres horizontal radius of a predetermined GPS location. The roundout results for the same five flights are shown in Figure 13. The entry location of the roundout control was specified as five metres altitude, although in reality the roundouts started slightly higher due to the ten metre radius applied to the GPS location at the end of the approach. The roundout is terminated upon the aircraft's airspeed dropping below $9m/s$ with the goal that the height above ground converged to two metres. In the flights the final heights ranged between 1.34m and 2.78m (mean of 2.1m standard deviation 0.6m), which in three of the landings provided very good results. The minimum and maximum points could have perhaps benefited from tighter control on height.

Finally upon the airspeed decaying to below $9m/s$ the flare control was initiated. Here a positive pitch rate of $60°/s$ was commanded until the aircraft reached 45°. Figure 14 shows the trajectories, including the commanded wing sweep angle (the actual position of the wing was not recorded). Due to the dynamics of the wing sweep mechanism and the tuning of the pitch rate controller, the pitch rate achieved actually overshot the commanded pitch rate. This pitch rate overshoot in this instance is not considered to be a problem as the $60°/s$ pitch rate was selected from flight experiments as a value that achieved good flare performance with the rate controller. Further analysis of the dynamics of the

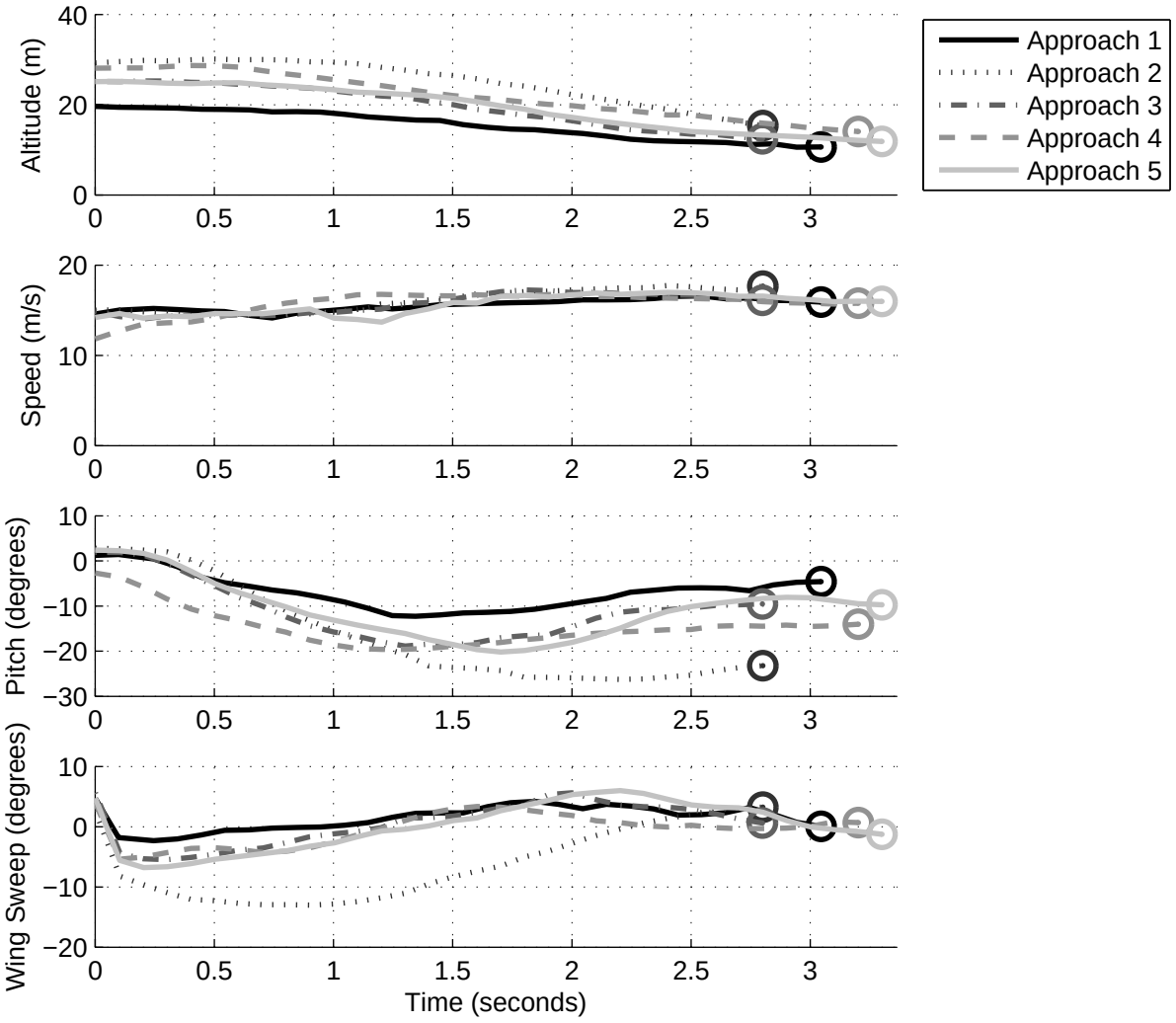

Figure 12: Aircraft data during five consecutive approaches

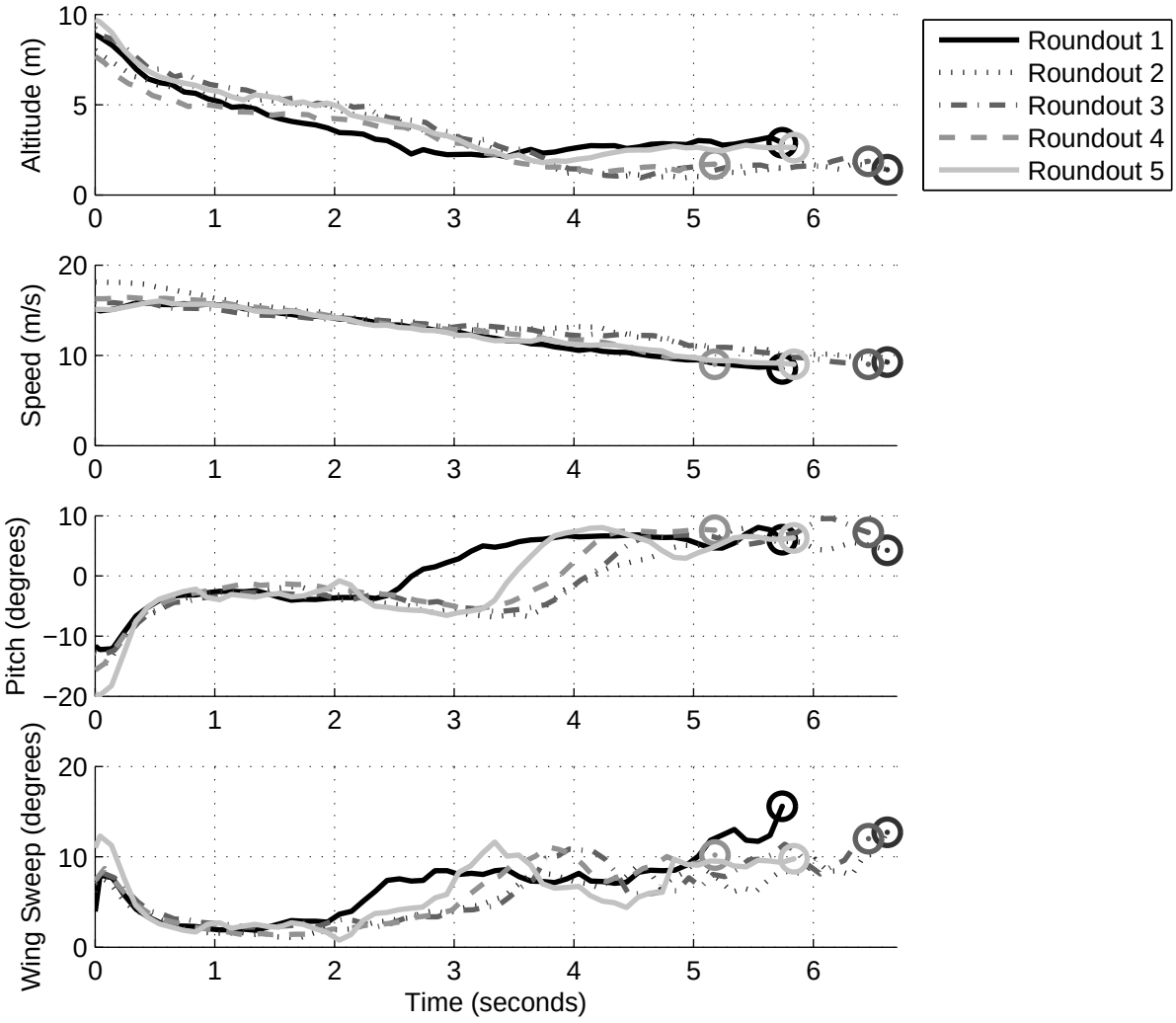

Figure 13: Aircraft data during five consecutive roundouts

wing sweep mechanism along with the pitch rate response could lead to tighter control here and then a different pitch rate would likely be commanded.

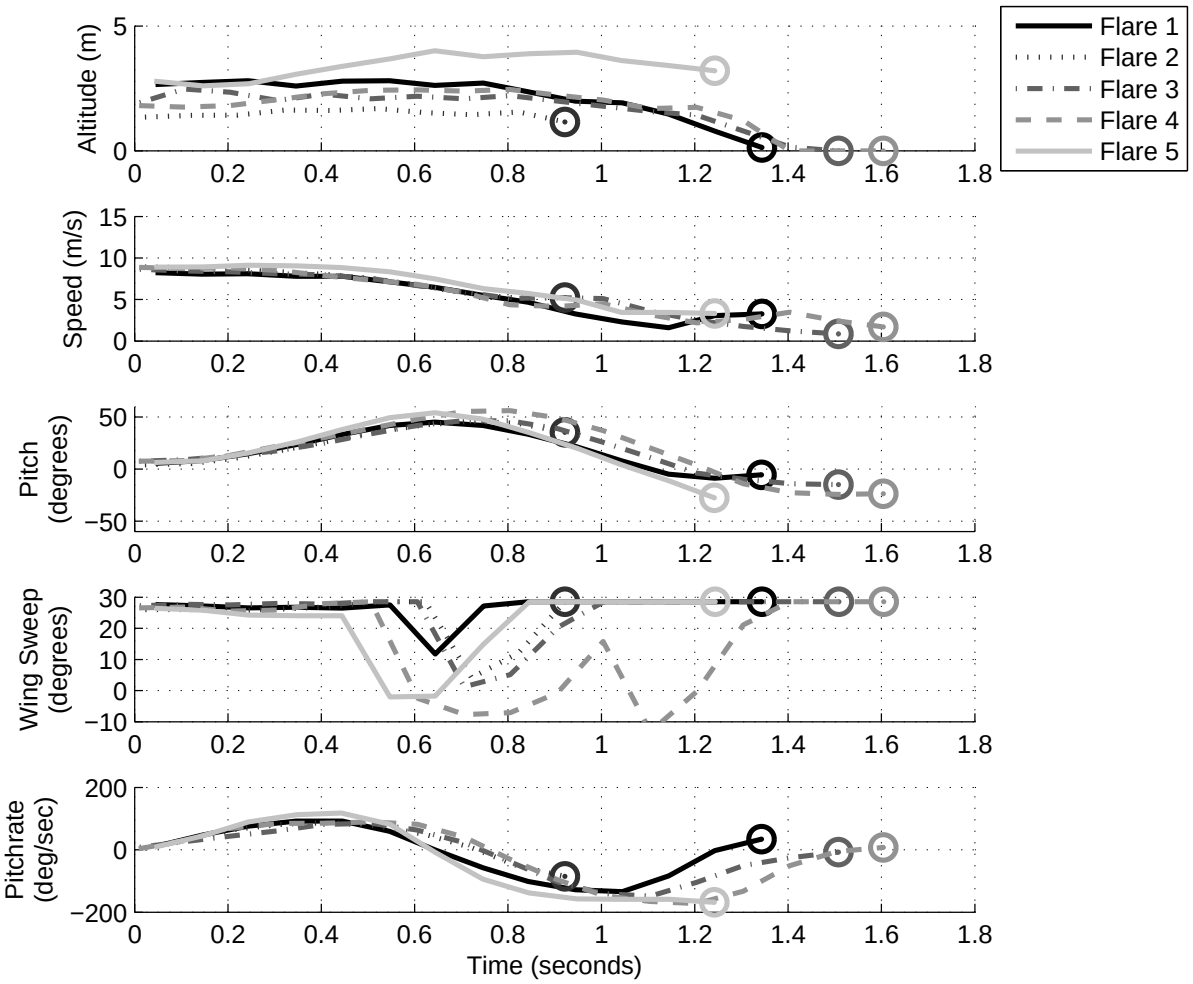

Figure 14: Aircraft data during five consecutive flare landings

The handover between the roundout controller and the flare controller was carefully constructed so that the flare was initiated at just the right speed and height. In reality this is a difficult guarantee to make. The pitch rate commanded should therefore be adjusted based upon entry speed as it is important to manage the potential and kinetic energy to achieve the final bleed off in airspeed whilst limiting the change in altitude. For example, in flight five the entry started high and the pitch rate achieved was also the highest of the five flights. The high pitch rate will have led to a delayed stall and the aircraft can be seen to ascend beyond its already high starting point. Additionally the airspeed is not seen to decay as quickly as in the other flights. This fifth flight was the only unsuccessful landing in that it terminated with the aircraft nose diving into the ground.

Although potentially not achievable, if the second flight had achieved a higher pitch rate then a lower landing speed may have been achieved. It was in this second flight that the flare began at a lower than expected height and so whilst the pitch and speed trajectories matched the other flights along with the altitude staying just as steady, the aircraft ended up touching down slightly early. Therefore it is expected that the robustness of the landing could be improved from developing the pitch rate controller

Flare No.	1	2	3	4	5
Initial Airspeed	$8.2m/s$	$8.9m/s$	$8.6m/s$	$8.9m/s$	$8.9m/s$
Initial Height	$2.7m$	$1.3m$	$1.9m$	$1.8m$	$2.8m$
Max. Pitch Rate	$92.1°/s$	$87.3°/s$	$84.9°/s$	$89.1°/s$	$118.0°/s$
Max. Pitch Angle	$45.2°$	$45.9°$	$46.6°$	$56.2°$	$54.1°$
Final Airspeed	$3.3m/s$	$5.2m/s$	$0.8m/s$	$1.7m/s$	$3.3m/s$
Note	Good	Landed early	Good	Good	Zoomed up

Table 2: Landing results from the five consecutive flare landings

based off analysis of the wing sweep and aircraft's pitch dynamics.

One peculiarity of the flare controller construction also worth discussing is due to the switch between rate hold and attitude hold for the pitch control. Upon reaching 45° the aircraft attempts to hold the attitude with a separate controller. When switching control laws the integrators are reset and the error between demand and measured pitch attitude is very low, which leads to a small sweep position being commanded. This small sweep angle can be seen by the brief dip in Figure 14 at around 0.7 seconds for four of the flights. The slight overshoot in pitch angle for flight four, however, means that the attitude controller has a bit more work to do in maintaining 45° and so the wing sweep time history varies.

Despite the reliance on the entry conditions the flare controller worked extremely well, demonstrating an ability to bring the aircraft from airspeeds just above the stall down to around $2m/s$ before finally touching down. The key results from the five flights are summarised in Table 2.

6. Conclusions

A variable sweep wing UAV was successfully designed, built and flown for perching manoeuvres onto flat ground. The custom wing box mechanism designed here was integrated with a modified off-the-shelf airframe. The aircraft demonstrated excellent reliability and robustness, which was ideal for developing new control laws and testing potentially dangerous manoeuvres such as perching. Pertinent aspects of the flight dynamics were discussed and wind tunnel data was presented that confirms the suitability of the airframe design and provides evidence for the theory behind the landing routines developed.

A new controller collection was developed for performing perched landings onto flat ground. Five consecutive landings were presented here with discussions on each of the three stages of the landing process. The approach and roundout segments were able to take the aircraft from the flight pattern where the altitude and speeds were seen to vary and deliver the aircraft at the start of the flare with a much tighter bounds on speed and height. The flare controller aimed for a fixed pitch rate to reduce the terminal airspeed. After performing the trials it is now thought that the pitch rate during this flare could, however, benefit from varying as a function of potential and kinetic energy in order to reduce the reliance on the strict entry conditions.

Acknowledgements

This research has been funded under the Autonomous System Underpinning Research programme from DSTL. The authors are grateful to Alan Davies from BAE Systems for helpful discussions during the project.

References

[1] J. Cooper, I. Chekkal, R. Cheung, C. Wales, N. Allen, S. Lawson, A. Peace, R. Cook, P. Standen, S. Hancock, *et al.*, "Design of a morphing wingtip," *Journal of Aircraft*, vol. 52, no. 5, pp. 1394–1403, 2015.

[2] M. Abdulrahim, "Flight performance characteristics of a biologically-inspired morphing aircraft," in *43rd AIAA Aerospace Sciences Meeting and Exhibit*, pp. 2005–345, 2005.

[3] D. Grant, M. Abdulrahim, and R. Lind, "Flight Dynamics of a Morphing Aircraft Utilizing Independent Multiple-Joint Wing Sweep," in *AIAA Atmospheric Flight Mechanics Conference and Exhibit*, American Institute of Aeronautics and Astronautics, 2006.

[4] S. Barbarino, O. Bilgen, R. M. Ajaj, M. I. Friswell, and D. J. Inman, "A review of morphing aircraft," *Journal of Intelligent Material Systems and Structures*, vol. 22, no. 9, pp. 823–877, 2011.

[5] A. R. Rodriguez, "Morphing aircraft technology survey," in *45th AIAA aerospace sciences meeting and exhibit*, pp. 2007–1258, 2007.

[6] T. Wyllie, "Parachute recovery for uav systems," *Aircraft Engineering and Aerospace Technology*, vol. 73, no. 6, pp. 542–551, 2001.

[7] H. J. Kim, M. Kim, H. Lim, C. Park, S. Yoon, D. Lee, H. Choi, G. Oh, J. Park, and Y. Kim, "Fully autonomous vision-based net-recovery landing system for a fixed-wing uav," *IEEE/ASME Transactions On Mechatronics*, vol. 18, no. 4, pp. 1320–1333, 2013.

[8] M. Kovac, "Learning from nature how to land aerial robots," *Science*, vol. 352, no. 6288, pp. 895–896, 2016.

[9] M. Kovač, J. Germann, C. Hürzeler, R. Y. Siegwart, and D. Floreano, "A perching mechanism for micro aerial vehicles," *Journal of Micro-Nano Mechatronics*, vol. 5, no. 3-4, pp. 77–91, 2009.

[10] M. Graule, P. Chirarattananon, S. Fuller, N. Jafferis, K. Ma, M. Spenko, R. Kornbluh, and R. Wood, "Perching and takeoff of a robotic insect on overhangs using switchable electrostatic adhesion," *Science*, vol. 352, no. 6288, pp. 978–982, 2016.

[11] H. Taniguchi, "Analysis of deepstall landing for uav," *Proceedings of ICAS2008, ICAS*, vol. 5, no. 4, p. 2008, 2008.

[12] S. H. Mathisen, K. Gryte, T. I. Fossen, and T. A. Johansen, "Non-linear model predictive control for longitudinal and lateral guidance of a small fixed-wing uav in precision deep stall landing," *AIAA SciTech*, 2016.

[13] R. E. Cory, *Supermaneuverable perching*. PhD thesis, Massachusetts Institute of Technology, 2010.

[14] J. Moore, R. Cory, and R. Tedrake, "Robust post-stall perching with a simple fixed-wing glider using lqr-trees," *Bioinspiration & Biomimetics*, vol. 9, no. 2, p. 025013, 2014.

[15] C. Meckstroth and G. W. Reich, *Near-Optimal Perching Trajectory Selection using Bézier Curve Interpolation*. American Institute of Aeronautics and Astronautics, 8 2013.

[16] D. V. Rao, H. Tang, and T. H. Go, "A parametric study of fixed-wing aircraft perching maneuvers," *Aerospace Science and Technology*, vol. 42, pp. 459–469, 2015.

[17] D. V. Rao and T. H. Go, "Perching trajectory optimization using aerodynamic and thrust vectoring," *Aerospace Science and Technology*, vol. 31, no. 1, pp. 1–9, 2013.

[18] A. Frank, J. S. McGrew, M. Valenti, D. Levine, and J. P. How, "Hover, transition, and level flight control design for a single-propeller indoor airplane," in *AIAA Guidance, Navigation and Control Conference and Exhibit*, p. 6318, 2007.

[19] M. R. Cutkosky, A. T. Abeck, and A. L. Desbiens, "Landing, perching and taking off from vertical surfaces," *The International Journal of Robotics Research*, vol. 30, no. 3, 2011.

[20] J. Thomas, G. Loianno, J. Polin, K. Sreenath, and V. Kumar, "Toward autonomous avian-inspired grasping for micro aerial vehicles," *Bioinspiration & biomimetics*, vol. 9, no. 2, p. 025010, 2014.

[21] M. Feroskhan and T. H. Go, "Dynamics of sideslip perching maneuver under dynamic stall influence," *Aerospace Science and Technology*, vol. 50, pp. 220–233, 2016.

[22] A. M. Wickenheiser and E. Garcia, "Optimization of perching maneuvers through vehicle morphing," *Journal of Guidance, Control, and Dynamics*, vol. 31, no. 4, pp. 815–823, 2008.

[23] K. Wright, *Investigating the Use of Wing Sweep for Pitch Control of a Small Unmanned Air Vehicle*. PhD thesis, University of California, San Diego, 2011.

[24] Z. R. Manchester, J. I. Lipton, R. J. Wood, and S. Kuindersma, "A variable forward-sweep wing design for improved perching in micro aerial vehicles," *55th AIAA Aerospace Sciences Meeting, AIAA SciTech Forum, (AIAA 2017-0011)*, 2017.

[25] "Pixhawk autopilot." `https://pixhawk.org/modules/pixhawk`.

[26] "Arduplane autopilot software." `https://github.com/diydrones/ardupilot`.

[27] A. A. Lambregts, "Vertical flight path and speed control autopilot design using total energy principles," *AIAA paper*, vol. 83, 1983.

[28] S. Park, J. Deyst, and J. P. How, "A new nonlinear guidance logic for trajectory tracking," in *Proceedings of the AIAA Guidance, Navigation and Control Conference*, pp. 1–16, 2004.

[29] "Arduplane autopilot software documentation." `http://plane.ardupilot.com/`.

[30] L. Faleiro and A. Lambregts, "Analysis and tuning of a 'total energy control system'control law using eigenstructure assignment," *Aerospace science and technology*, vol. 3, no. 3, pp. 127–140, 1999.

[31] B. L. Stevens and F. L. Lewis, *Aircraft control and simulation*, vol. 2. Wiley New York, 2003.